Atmospheric Environment 286 (2022) 119221

Contents lists available at ScienceDirect

Atmospheric Environment

journal homepage: www.elsevier.com/locate/atmosenv

Characterisation of non-exhaust emissions from road traffic in Lisbon

I. Cunha-Lopes [a,*], C.A. Alves [b], I. Casotti Rienda [b], T. Faria [a], F. Lucarelli [c], X. Querol [d], F. Amato [d], S.M. Almeida [a]

[a] Centro de Ciências e Tecnologias Nucleares, Instituto Superior Técnico, Universidade de Lisboa, Estrada Nacional 10, 2695-066, Bobadela-LRS, Portugal
[b] Centre of Environmental and Marine Studies, Department of Environment, University of Aveiro, 3810-193, Aveiro, Portugal
[c] INFN - Firenze, National Institute for Nuclear Physics - Florence Division, 50019, Sesto Fiorentino, Italy
[d] Institute of Environmental Assessment and Water Research, Spanish Research Council (IDÆA-CSIC), 08034, Barcelona, Spain

HIGHLIGHTS

- Non-exhaust emissions have an important impact on the environment and health.
- Cobbled pavement had a higher dust load than asphalt pavements.
- Cu revealed the highest potential ecological harmful effect.
- Cu and Zn revealed an extremely high pollution index in all road sampling sites.
- Exposure to As may contribute to the development of cancer over a lifetime.

GRAPHICAL ABSTRACT

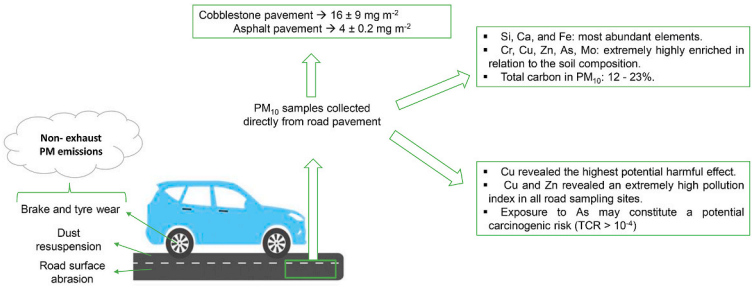

ARTICLE INFO

Keywords:
Non-exhaust emissions
PM_{10}
OC/EC
Metals
Pollution indexes
Health risks

ABSTRACT

Non-exhaust emissions from road transport include particles from brake and tyre wear, road surface abrasion and dust resuspension. Road dust loads and their chemical properties are heterogeneous and their knowledge is still scarce. This study aimed to characterise, for the first time in Lisbon, the thoracic fraction of road dust (PM_{10}) by collecting samples directly from road pavements by an *in situ* resuspension chamber. The highest PM_{10} load (15.6 ± 8.75 mg m^{-2}) was obtained on a cobblestone pavement, while for asphalt roads the mean PM_{10} load was 4.40 ± 0.16 mg m^{-2}. Emission factors for asphalt pavements ranged from 83.5 to 274 mg veh^{-1} km^{-1}. On average, 65.7% of the PM_{10} mass was reconstructed, taking into account the carbonaceous content and the sum of the elements in their oxidized form. Cu and Zn, associated with brake and tyre wear, were the most enriched elements in relation to the soil composition (EnF = 440 and 184, respectively). The highest potential ecological risk factor of individual metals (Eri) was also observed for Cu (Eri_{Cu} = 393). In 90% of the sampled streets, the total carcinogenic risk was higher than 1E-4 for As, suggesting that exposure to this hazardous element may contribute to the development of cancer over a lifetime. The results showed the high contribution of certain dangerous chemical compounds associated with resuspension particles and their potential effects on human health.

* Corresponding author.
E-mail address: ines.lopes@ctn.tecnico.ulisboa.pt (I. Cunha-Lopes).

https://doi.org/10.1016/j.atmosenv.2022.119221
Received 27 December 2021; Received in revised form 31 May 2022; Accepted 4 June 2022
Available online 8 June 2022

1. Introduction

Airborne particulate matter with aerodynamic diameter below 10 and 2.5 μm (PM_{10} and $PM_{2.5}$, respectively) is one of the major environmental risks with harmful effects on human health (Almeida et al., 2014; EEA, 2019; Kelly and Fussell, 2011). In 2018, it was estimated that about 417,000 people died prematurely due to exposure to $PM_{2.5}$ in Europe (EEA, 2020).

Almost three quarters of the European Union's population lives in urban areas (Eurostat, 2016) and this is where the highest traffic density occurs. In urban areas, vehicle emissions are one of the major sources of air pollutants, mainly PM (Amato et al., 2016a; Byčenkiene et al., 2014; Custódio et al., 2016; Pant and Harrison, 2013), being the second largest contributor to primary $PM_{2.5}$ and black carbon (BC) (EEA, 2019). Road transport emissions comprise exhaust emissions from internal combustion engines and non-exhaust emissions. The latter include particles from brake and tyre wear, road surface abrasion and dust resuspension from weathered materials of pavements, diesel and gasoline engine exhausts, lubricating oils and atmospherically deposited materials from non-vehicular emissions (Alves et al., 2018; Thorpe and Harrison, 2008). In particular, road dust resuspension may account for a substantial fraction of non-exhaust emissions. In addition to meteorological patterns (Amato et al., 2017), road dust properties vary with the type of pavement (Gustafsson et al., 2019) and traffic conditions, such as intensity (Pant and Harrison, 2013), vehicle properties (e.g., vehicle mass and size, brake and tyre material) (Farwick zum Hagen et al., 2019; Oroumiyeh and Zhu, 2021) and driver behaviour (braking intensity, acceleration/deceleration modes) (Amato et al., 2017; Oroumiyeh and Zhu, 2021). Depending on these conditions, road dust can represent a share of up to 60% of non-exhaust emissions, which, in turn, predominate over exhaust emissions, as a result of restrictive measures and technological advances in the automotive sector (Casotti Rienda and Alves, 2021). Furthermore, any source of PM can contribute to road dust accumulation by deposition. Therefore, the loads and chemical properties are heterogeneous and emission factors differ from location to location (Alves et al., 2018; Amato et al., 2017; Bukowiecki et al., 2010). Thus, to more accurately account for the contribution of this source in emission inventories and receptor models, locally available emission factors and chemical fingerprints should be used.

Road dust may contain harmful components, such as metals and polycyclic aromatic hydrocarbons (PAHs) (Alves et al., 2018; Li et al., 2015; Yu et al., 2020; Zhang and Wang, 2009; Zhao et al., 2009), which may induce toxicological responses (Cho et al., 2018; Huang et al., 2015; Koh and Kim, 2019) and multiple health effects, especially on the respiratory and cardiovascular systems (Khan and Strand, 2018). The toxicity of non-exhaust emissions, and in particular of road dust, is scarcely known (Dumax-Vorzet et al., 2015; Huang et al., 2015; Koh and Kim, 2019). The toxicological properties of road dust particles are highly variable and dependent on their chemical characteristics (Candeias et al., 2020; Casotti Rienda and Alves, 2021). .

Non-exhaust emissions are an increasing concern since there is no policy for this type of emission. This paper aims to obtain emission factors and chemically characterise the thoracic fraction of road dust (PM_{10}) for the first time in Lisbon, the capital of Portugal. From the climatic point of view, Portugal is a Mediterranean country, where dry weather conditions and long periods without precipitation can occur, which can favor the accumulation and consequent resuspension of road dust. These results can contribute to European emission inventories and source apportionment models, to assess the impact of traffic generated PM on both human health and the environment, and to help implement mitigation and control measures.

2. Materials and methods

2.1. Study area

Lisbon is the largest city of Portugal with a population density of 951 inhabitants km^{-2} in 2020. The dominant source of air pollution is road traffic (Almeida et al., 2009). According to data available for the district of Lisbon, the number of vehicles in 2020 was 1,628,108, of which 87.7% were light-duty vehicles (ASF, 2020).

Road dust was collected from six roads in the city of Lisbon, chosen together with the municipal authorities to represent different traffic patterns and environments in the city (Table 1). The description of the traffic classification (high and low traffic) at each sampling site was categorized based on *a priori* knowledge of the area. The city centre has higher levels of traffic, while the residential area has low traffic.

Fig. 1 shows the geographic location of the sampling areas. Streets with asphalt and granite cobblestone were analysed because they represent the two types of pavement existing in Lisbon. In addition, for asphalt, which is the predominant pavement, samples were taken from the streets and two main tunnels in Lisbon.

2.2. Road dust sampling

Measurements were performed in surface areas of 1 m^2 for 30 min each. Sampling areas were selected on the right lane of the street excluding the gutter where mass is not directly resuspended. In each road, three different square meters were sampled using three different filters of 47 mm diameter (one PTFE with 2.0 μm pore size from Whatman®, and two quartz fibre filters from Pallflex®). Thus, 18 samples were collected in total. Two different types of filters were used to perform specific chemical analyses on each matrix, as explained in subchapter 2.3.2.

Road dust collection took place in autumn 2020 in just one day to obtain samples under the same meteorological conditions. No precipitation was registered in the days before and during the sampling campaign. The sampling protocol involved the support of the police authorities for the whole duration of the campaign to supervise traffic and guarantee safety.

Road dust samples were collected directly from the road pavement with an *in situ* resuspension chamber (Fig. 2) (Amato et al., 2009b) that vacuumed the material deposited on the pavements at an air flow rate of 25 L min^{-1}, using a rotary vane pump (Thomas, Picolino VTE Series). Dust was immediately resuspended in a methacrylate deposition chamber and particles small and/or light enough to be carried by the air current continued their trip through the system. These particles entered a *Negretti* stainless steel elutriation filter designed to only allow the passage of particles <10 μm. The particles able to penetrate this barrier were finally collected on the filter, while particles with aerodynamic

Table 1
Location and type of pavement of the sampling points.

Sampling points	Location	Description	Type of pavement
S1	Manuel Jesus de Coelho Street, next to Liberdade Av.	High traffic; city core	Asphalt
S2	Artilharia 1 Street, Campolide	High traffic; city core	Cobbled
S3	Forças Armadas Av., Entrecampos	High traffic; after a roundabout; city core	Asphalt
S4	Padre António Proença Av., Benfica	Low traffic; residential area	Asphalt
S5	João XXI tunnel, Campo Pequeno	Tunnel with high traffic; city core	Asphalt
S6	Marquês tunnel, Marquês de Pombal	Tunnel with high traffic; heavy vehicles are not allowed; city core	Asphalt

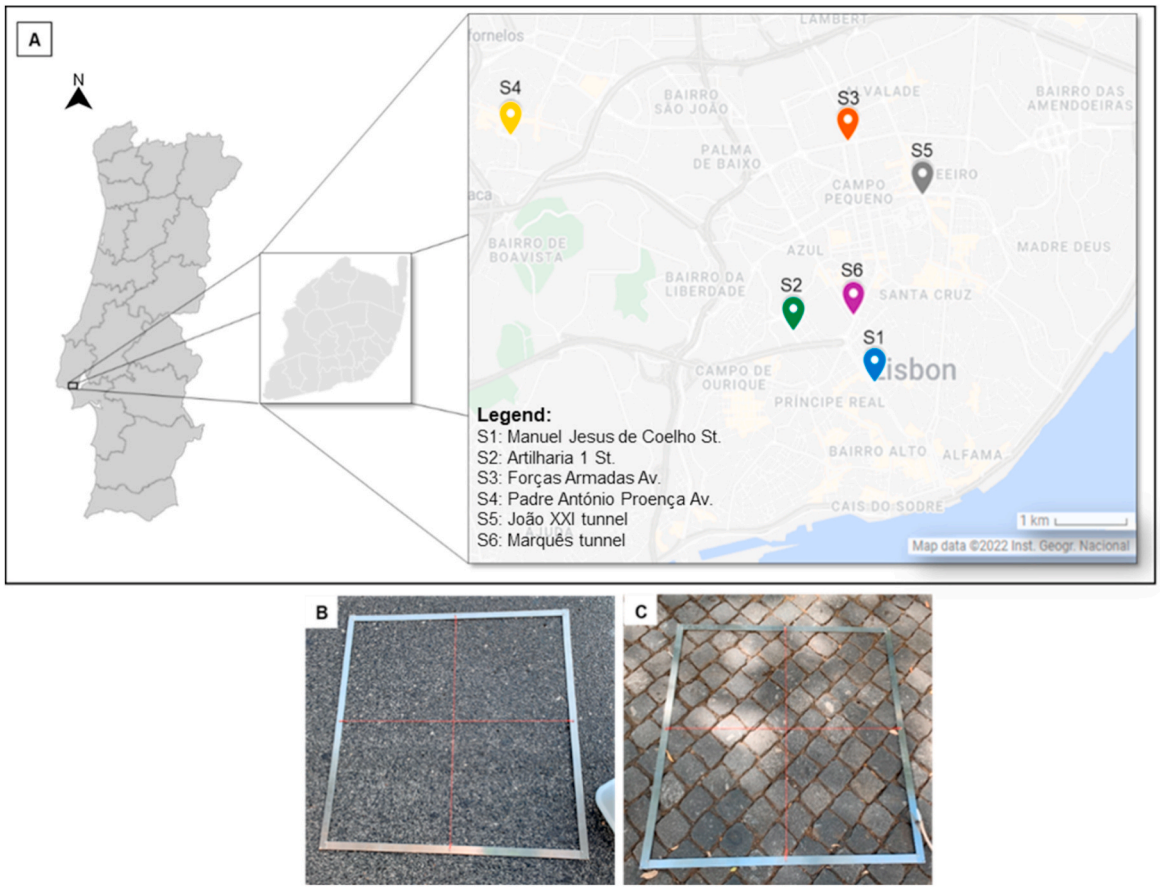

Fig. 1. A: Geographic location of the sampling points in Lisbon: S1 - high traffic, asphalt; S2 - high traffic, cobbled; S3 - high traffic, asphalt; S4 - low traffic, asphalt; S5 - tunnel high traffic, asphalt; S6 - tunnel high traffic without heavy vehicles, asphalt; B: Asphalt pavement; C: Cobbled pavement.

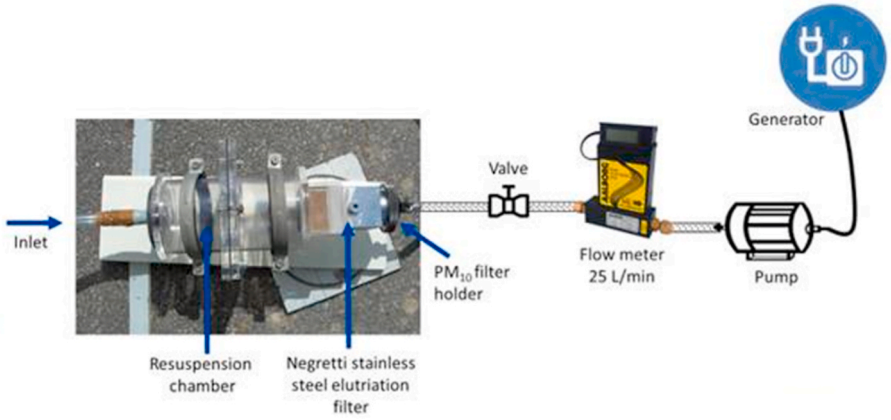

Fig. 2. Road dust *in situ* resuspension chamber and sampling train to collect PM_{10}.

diameter >10 μm were deposited in the methacrylate chamber and along the elutriation filter.

2.3. Analytical determinations

2.3.1. PM mass concentrations

Quartz filters were calcined at 500 °C for 6 h and were conditioned for around 24 h in a room with controlled humidity (50%) and temperature (20 °C) before the first weighing.

Filters used in the dust sampling device were weighed before and after sampling by means of a microbalance following the procedure described in EN12341 (EU, 2008). After sampling and weighing, the filters were stored in a freezer at - 20 °C until the chemical analysis.

2.3.2. Chemical analysis

2.3.2.1. Elemental composition. PM was chemically analysed for major and trace elements. PTFE filters were cut in two sections and half of each filter was analysed by particle induced X-ray emission (PIXE), described by Lucarelli et al. (2018), for the measurement of the elements with atomic number higher than 10 (Na, Mg, Al, Si, P, S, Cl, K, Ca, Ti, V, Cr, Mn, Fe, Ni, Cu, Zn, As, Se, Br, Rb, Sr, Y, Zr, Mo, Ba and Pb). PIXE

measurements were done at INFN LABEC using a 3 MeV proton beam extracted into ambient pressure and the Ketek Silicon Drift Detector (SDD) array available at the external beam PIXE facility for atmospheric aerosol analysis. The data analysis was performed using the GUPIXWIN software (Campbell et al., 2010).

2.3.2.2. Carbonaceous content. PM_{10} quartz filters were analysed by a thermal-optical transmittance technique for the determination of organic carbon (OC) and elemental carbon (EC). This method was previously described by Pio et al. (2011). Firstly, the organic fraction of the particles is vaporized in a nitrogen atmosphere up to 600 °C. EC is determined by sequential heating to 850 °C in an atmosphere containing 4% oxygen. The carbon released in the various steps, in the form of CO_2, is quantified by a non-dispersive infrared (NDIR) analyzer. Monitoring of the light transmittance through the filter with a laser beam allows correcting the EC formed by pyrolysis of the OC during the first heating step from the one that was originally present in the filter.

The concentration of OC and EC was normalized to the PM_{10} concentration of PTFE samples since the carbonaceous content were analysed in quartz filters and the elements in PTFE filters.

2.4. Mass closure

Mass closure was made to determine the contribution of possible emission sources to the total PM_{10} mass, taking into account the gravimetric measurements and the sum of directly or indirectly determined PM_{10}-bound constituents (Table 2).

Elements were grouped into three main emission sources: mineral dust (MD), sea salt (SS), and anthropogenic (Anthrop.) based on the enrichment factors (section 2.6.1) and a table by Calvo et al. (2013), in which source specific inorganic marker elements are summarized. The mass balance also included particle organic matter (POM), EC, and unidentified matter (UM). The latter includes unanalysed constituents, as well as unaccounted particle-bound water.

As concerns the mass balance, all elements were considered, including values below the detection limit, which were substituted by half of its value.

POM was estimated by multiplying OC by a factor of 1.9 since thermal–optical analytical techniques are unable to measure elements other than carbon, such as oxygen, nitrogen, sulfur, hydrogen, chlorine and other species associated with the organic mass (Polidori et al., 2008). Sea salt was calculated based on major sea salt components and typical elemental ratios for sea water as Mg/Na = 0.119, K/Na = 0.0370, Ca/Na = 0.0380 and SO_4^{2-}/Na = 0.253 (Almeida et al., 2006; Calzolai et al., 2015). For MD, the soil fractions of Mg, K, Ca, Fe and Ba have been calculated using their typical crustal ratios with respect to aluminum (Wedepohl, 1995): Mg/Al = 0.170, K/Al = 0.370, Ca/Al = 0.380, Fe/Al = 0.400 and Ba/Al = 0.0100. For the anthropogenic sources, Mg, K, Ca, Fe, and Ba with anthropogenic origin were calculated using the following equation: [anthrop.X] = [TotalX] - [ssX] - [soilX], where X is the element. For MD and Anthrop., the presence of common oxides was assumed, so element concentrations were multiplied by a factor to account for the oxygen mass (Table S1).

2.5. Emission factors

Emission Factors (*EFs*) were calculated for vehicular non-exhaust emissions. To estimate the *EFs* (mg km^{-1} veh^{-1}) of PM_{10} road dust resuspension, the empirical relationship derived by Amato et al. (2011) was used.

$$\boldsymbol{EF} = 45.9 \ \mathbf{x} \ \boldsymbol{RD}^{0.81} \quad (1)$$

where *RD* (mg m^{-2}) is the deposited loadings of PM_{10}.

2.6. Pollution indexes

2.6.1. Enrichment factor

The enrichment factor for each element was calculated to assess the presence and intensity of road dust contamination by anthropogenic sources (Yang et al., 2016).

$$\boldsymbol{EnF} = \frac{[\boldsymbol{C_n}/\boldsymbol{C_{ref}}]_{\mathbf{sample}}}{[\boldsymbol{C_n}/\boldsymbol{C_{ref}}]_{\mathbf{UCC}}} \quad (2)$$

where C_n is the concentration of an element and C_{ref} is the concentration of the reference crustal element. In this study, the element Al was used as the reference for normalization of the crustal element (Almeida et al., 2005). UCC represents the average upper continental crust. The values of Wedepohl (1995) were used (Table S2), since standard background values for soil and dust are not available for Portugal. According to Yang et al. (2016), five contamination categories can be recognized – $EnF < 2$: minimal enrichment; $2 \leq EnF < 5$: moderate enrichment; $5 \leq EnF < 20$: significant enrichment; $20 \leq EnF < 40$: very high enrichment; $EnF \geq 40$: extremely high enrichment.

2.6.2. Potential ecological risk and pollution load index

The potential ecological risk factor of individual metals (*Eri*) was calculated as follows (Zgłobicki et al., 2019):

$$\boldsymbol{Eri} = \boldsymbol{T_i} \times \boldsymbol{PI} \quad (3)$$

where *Ti* is the toxic-response factor for the metal, which was taken from Hakanson (1980): As, 10; Cu, 5; Ni, 5; Pb, 5; Cr, 2; V, 2; Zn, 1; Mn, 1; Ba, 1. *PI* is the pollution index to assess the level of contamination of metals in dust (Lee et al., 2006). *PI* is obtained by:

$$\boldsymbol{PI} = \boldsymbol{C_n}/\boldsymbol{B_n} \quad (4)$$

According to Wu et al. (2014), *PI* can be classified into five groups – $PI < 1$: low; $1 \leq PI < 3$: moderate; $3 \leq PI < 6$: considerable; $6 \leq PI < 12$: very high; $PI \geq 12$: extremely high.

The integrated pollution load index (*PLI*) was calculated to evaluate the overall pollution status and to specify the contamination degree. It is obtained by the following equation:

$$\boldsymbol{PLI} = (\boldsymbol{PI}_1 \times \boldsymbol{PI}_2 \times \ldots \times \boldsymbol{PI}_n)^{1/\mathbf{n}} \quad (5)$$

where n is the number of elements analysed. *PLI* can be categorized into 7 groups (Zhang et al., 2011) – $PLI = 0$: background concentration; $0 < PLI \leq 1$: unpolluted; $1 < PLI \leq 2$: unpolluted to moderately polluted; $2 < PLI \leq 3$: moderately polluted; $3 < PLI \leq 4$: moderately to highly

Table 2
Elements associated with emission sources.

POM	1.9 × [OC]
Sea Salt	[Na] + [Cl] + [ssMg] + [ssK] + [ssCa] + [ssSO$_4^{2-}$]
Mineral Dust (MD)	[Al] + [Si] + [Ti] + [P] + [Mn] + [soilMg] + [soilK] + [soilCa] + [soilFe] +[soilBa] + [Sr]
Anthropogenic	[anthrop.Mg] + [anthrop.K] + [anthrop.Ca] + [anthrop.Fe] + [V] + [Cr] + [Ni] + [Cu] + [Zn] + [As] + [Se] + [Br] + [Rb] + [Y] + [Zr] + [Mo] + [anthrop.Ba] + [Pb] + [anthrop.SO$_4^{2-}$]

polluted; $4 < PLI \leq 5$: highly polluted; $PLI \geq 5$: very highly polluted.

The potential ecological risk factor, *Eri*, can be classified in 5 groups (Hakanson, 1980) – $Eri < 40$: low; $40 \leq Eri < 80$: moderate; $80 \leq Eri < 160$: considerable; $160 \leq Eri < 320$: high; $Eri \geq 320$: very high.

The multiple risk (*RI*) is the result of the sum of individual *Eri* values for the n metals in a sample, as follows:

$$RI = \sum_{i=1}^{n} Eri \tag{6}$$

It can be categorized as – $RI < 150$: low; $150 \leq RI < 300$: moderate; $300 \leq RI < 600$: considerable; $RI \geq 600$: high (Hakanson, 1980).

2.7. Human health risk assessment

Humans can be exposed to metals in road dust particles by ingestion, inhalation and dermal contact. To assess the human exposure risk, the average chronic daily dose from soil by ingestion, dermal and inhalation absorption are CDD_{ing}, CDD_{derm} and CDD_{inh}, respectively. The methodology applied in this study was defined by the United States Environmental Protection Agency (USEPA, 1989). Chronic daily doses were calculated by Eqs. (7)–(9) (Adimalla, 2020; Chen et al., 2015; and references therein).

$$CDD_{ing} = C_n \times \frac{IR_{ing} \times EFreq \times ED}{BW \times AT} \times 10^{-6} \tag{7}$$

$$CDD_{derm} = C_n \times \frac{SA \times SAF \times DAF \times EFreq \times ED}{BW \times AT} \times 10^{-6} \tag{8}$$

$$CDD_{inh} = C_n \times \frac{IR_{inh} \times EFreq \times ED}{PEF \times BW \times AT} \tag{9}$$

where C_n is the concentration of a specific metal in road dust (mg kg^{-1}), IR_{ing} is the ingestion rate of dust (100 mg day^{-1} for adults and 200 mg day^{-1} for children) and IR_{inh} is the inhalation rate of dust (12.8 m^3 day^{-1} for adults and 7.63 m^3 day^{-1} for children), *EFreq* is the exposure frequency (365 days $year^{-1}$), *ED* is the exposure duration (30 years for adults and 6 years for children), *BW* is the average body weight of the exposed individual (70 kg for adults and 20 kg for children), *AT* is the average time for non-carcinogens (*ED* x 365 days) and for carcinogens (As, Cr, Ni, and Pb; $AT = 70 \times 365$ days), *SA* is the exposed skin surface area (4350 cm^2 for adults and 1600 cm^2 for children), *SAF* is the skin absorption factor (0.7 mg cm^2 for adults and 0.2 mg cm^2 for children), *DAF* is the dermal absorption factor (0.001 for adults and children) and *PEF* is the particle emission factor (1.36E9 m^3 kg^{-1}).

2.7.1. Carcinogenic and non-carcinogenic risk

The possibility of an individual develop any type of cancer in the whole lifetime due to exposure to carcinogenic hazards is called the carcinogenic risk (*CR*) and can be calculated as (Adimalla, 2020; and references therein):

$$CR_n = CDD \times SF \tag{10}$$

where CR_n is the carcinogenic risk for a specific metal (As, Cr, Ni and Pb) and *SF* is the slope factor, which is an upper bound, approximating a 95% confidence limit, on the increased cancer risk from a lifetime exposure to a chemical. It is calculated by looking at toxicology data on how cancer risk rises with increased exposure to a certain compound and is expressed in mg kg^{-1} day^{-1}. The *SF* values adopted in this study were taken from the bibliography (Table S3). The CR_{As} was the only one for which all the three exposure modes were considered in the model, because of the unavailability of *SF* values for various metals and exposure routes. It was possible to calculate CR_{Pb} values for the ingestion and dermal routes, while for CR_{Cr} and CR_{Ni} only inhalation was considered (Ferreira-Baptista and De Miguel, 2005; USEPA, 1989). The total carcinogenic risk (*TCR*) is the sum of *CR* values for each n single metal of each sampling site:

$$TCR = \sum CR_{n\_dermal} + CR_{n\_ingestion} + CR_{n\_inhalation} \tag{11}$$

Values < 1E-6 are regarded as negligible, values between 1E-6 and 1E-4 are taken as acceptable or tolerable cancer risks, and values > 1E-4 are considered to be likely harmful to human health (USEPA, 1989). To assess the non-carcinogenic risk, the hazard quotient (*HQ*) was calculated by the following equation:

$$HQ_n = CDD / R_fD \tag{12}$$

where *CDD* is the chronic daily dose and R_fD (mg day^{-1} kg^{-1}) is the reference dose for a given substance (Table S3) (Adimalla, 2020; and references therein). The hazard index (*HI*) is the sum of individual HQ_n values and represents the total risk of non-carcinogenic elements via three exposure pathways (HQ_{ing}, HQ_{inh} and HQ_{derm}). If $HI < 1$, no risk of noncarcinogenic effects is believed to occur, while a $HI > 1$ indicates that potential non-carcinogenic effects on humans can take place.

3. Results and discussion

3.1. PM_{10} road dust loadings and emission factors

The PM_{10} mass fraction for each sampling point was obtained by averaging the three different square meters analysed at each location. PM_{10} road dust load was on average 6.27 ± 2.35 mg m^{-2} (ranging from 2.09 to 15.6 mg m^{-2}) for the six sampling sites. In detail, as shown in Fig. 3, the sampling site with the highest load of PM_{10} (15.6 ± 8.75 mg m^{-2}) was Artilharia 1 Street (S2), which has a cobblestone pavement. The PM_{10} load was, on average, 4.40 ± 0.16 mg m^{-2}, for the asphalt pavements. Higher loads of PM_{10} for cobblestone pavements compared to asphalt roads were also found in previous studies, as in the case of Oporto and Paris, where the dust loads were about 50 and 10 times higher for paving stones, respectively (Alves et al., 2018; Amato et al., 2016b). Since cobblestone pavements are made with granite cubes, the roughness is greater, favoring the deposit of particulate material. On the other hand, during sampling, the soil material that fills the joints can be vacuumed, leading to higher dust loads (Alves et al., 2018, 2020).

In comparison with other studies, the mean values obtained are similar to those reported for Spanish cities, such as in Girona and Barcelona, where PM_{10} road dust loads varied from 1.3 to 7.1 mg m^{-2} and

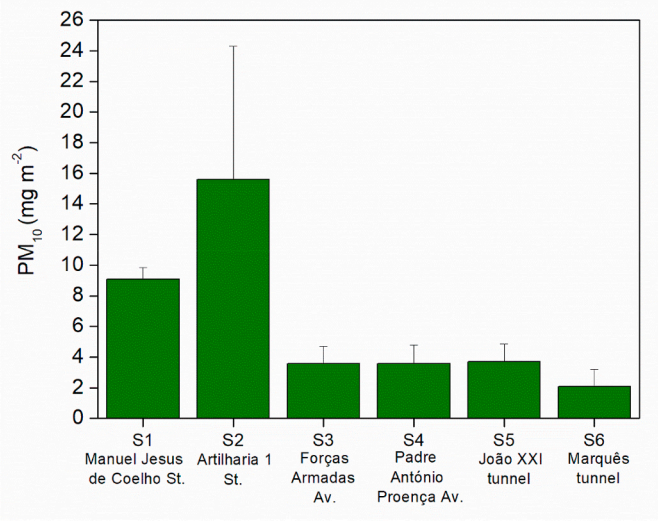

Fig. 3. Load of PM_{10} mass fraction of road dust per m^2 of each sampling point. (S1: high traffic, asphalt; S2: high traffic, cobbled; S3: high traffic, asphalt; S4: low traffic, asphalt; S5: tunnel high traffic, asphalt; S6: tunnel high traffic without heavy vehicles, asphalt).

from 3 to 23 mg m^{-2}, respectively (Amato et al., 2009b, 2011, 2009b). In city centres, traffic is dense but vehicles circulating in these locations are mainly passenger cars, motorcycles and light commercial vehicles, while other roadways can be more affected by the fugitive dust released by uncovered heavy trucks (Amato et al., 2009b). This study recorded average levels higher than those documented for Paris, where PM_{10} road dust loads ranged from 0.7 to 2.2 mg m^{-2} (Amato et al., 2016b). Mean values of 0.48 ± 0.39 mg m^{-2} and 1.06 mg m^{-2} for asphalt pavements were registered in Oporto and Viana do Castelo, in Portugal, respectively, for the same road dust granulometric fraction (Alves et al., 2018, 2020). In these two latter locations, some streets were washed in the night before and/or in the morning before sampling, which may have led to a reduction of road sediments, since water adheres to deposited particles reducing the likelihood of suspension and transport (Watson et al., 2000). Some studies have already demonstrated that street washing can be a potentially effective measure to reduce road dust loads. Alves et al. (2020) documented an 83% efficiency in reducing dust on the roads after high pressure washing and sweeping. Other examples of measures that can reduce the load of PM_{10} on urban roads are awareness campaigns to encourage vehicle sharing and promote the use of public transport and bicycles, thus allowing fewer cars to circulate in the city.

PM road dust varies from place to place, as it depends on several factors, such as type of pavement, road pavement wear, brake pad and tyre formulations, handling of dusty materials (e.g., demolishing) and also the local weather, since it influences the deposition, accumulation, adherence to the pavement surface and withdrawal of particles (Zhao et al., 2006; Han et al., 2007; Amato et al., 2009a, b; Casotti Rienda and Alves, 2021).

The mean *EF* obtained by Eq. (1) ranged between 83.5 and 274 mg veh^{-1} km^{-1} for asphalt pavements. A mean value of 425 mg veh^{-1} km^{-1} was derived for the cobbled pavement. The *EF* reported for Barcelona was 97 mg veh^{-1} km^{-1} (Amato et al., 2010), whilst in Oporto mean values ranged from 12.9 to 29.4 mg veh^{-1} km^{-1} for asphalt roads and was 1082 mg veh^{-1} km^{-1} for a cobbled pavement (Alves et al., 2018).

3.2. Chemical characterisation

3.2.1. Mass closure

The mass closure analysis was a first approach to estimate the contribution of possible sources to the PM_{10} road dust (Fig. 4). To allocate chemical constituents to general sources, information from previous studies was used (Calvo et al., 2013; Diapouli et al., 2017).

On average, the chemical constituents, including elements in their oxidized form (such as Al_2O_3, MgO, Fe_2O_3, TiO_2, K_2O, etc.), organic matter and elemental carbon, accounted for 65.7% (69.1% and 48.7% of the PM_{10} mass for asphalt pavements and cobbled pavement, respectively) of the PM_{10} mass of road dust. Therefore, unidentified/unquantified constituents and particle-bound water represented a PM_{10} mass fraction of about 34.3%. Taking into account the identified matter, Fig. 4 shows that anthropogenic elements (22.0%), POM (19.8%) and mineral dust (15.7%) are the sources that predominantly contribute to the total PM_{10} mass, followed by EC (7.77%) and sea salt (0.49%).

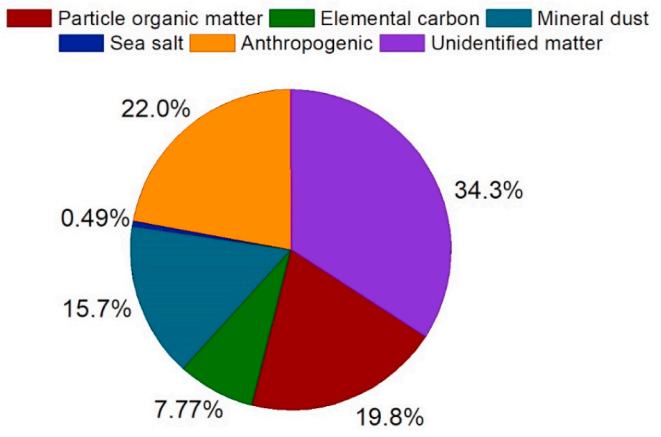

Fig. 4. Mass closure of the PM_{10} fraction of road dust. Average of the six sampling points.

3.2.2. OC/EC and elements

The carbonaceous and elemental content in the PM_{10} fraction of road dust is shown in Table 3. This information can contribute to the European database SPECIEUROPE for non-exhaust emissions and be useful to constrain source apportionment studies. The sum of major and trace elements accounted for 16.9–28.1% of the PM_{10} mass.

The average metal mass fractions (wt %) of Cr (0.0279 ± 0.0178), Cu (0.112 ± 0.0784), Zn (0.172 ± 0.0670), As (0.00182 ± 0.000720) and Mo (0.00694 ± 0.00336) in urban street dust were much higher than the soil background values. Previous studies, namely in Viana do Castelo (Alves et al., 2020) and Barcelona (Amato et al., 2011), have identified the elements Cr (0.0296 ± 0.0281% and 0.0237 ± 0.0105%, respectively), Cu (0.182 ± 0.114% and 0.139 ± 0.0705%, respectively) and Zn (0.216 ± 0.115% and 0.153 ± 0.0440%, respectively) as common tracers of non-exhaust emissions. The crustal elements Ca (10.7 ± 1.51%), Si (4.66 ± 0.861%) and Fe (4.65 ± 2.60%) were the most abundant. Ca represented high PM_{10} mass fractions. Construction-related and asphalt-derived particles have also been pointed out as sources of crustal materials in road dust (Legret et al., 2005; Wiseman et al., 2021; Zhang et al., 2005). In Lisbon, one must also take into account that part of the city's geology is made up of limestone (Mendonça, 2016) and its sidewalks are made of cubes of this rock. Previous studies have also reported high Ca abundances in road dust. Amato et al. (2011) reported in three European cities Ca mass fraction of 8.1 ± 3.7% in Zürich, 13.2 ± 4.75% in Barcelona and 20.6 ± 9.1% in Girona. In Viana do Castelo, Si, Al, Fe, Ca and K were also the most abundant elements. In this latter study, Ca mass fraction was 2.27 ± 2.00%, but the geology of Viana do Castelo (North of Portugal) is granitic.

Road dust comprises various organic compounds from vehicular and non-vehicular origins, such as exhaust emissions, lubricating oils, tyre and brake debris, and also from atmospherically deposited materials (Alves et al., 2018; Amato et al., 2011). According to Amato et al. (2011), EC and OC are the main components of vehicular exhaust, but OC is also associated with tyre wear. In this study, the percentage of total carbon (TC = OC + EC) in PM_{10} ranged between 11.9 and 23.2%. Mean EC and OC mass fractions of 7.84 ± 0.03% and 10.38 ± 0.03% were obtained, respectively. Lower OC mass fractions were observed in Oporto and Viana do Castelo (7.1 ± 3.5% and 5.6 ± 1.2%, respectively). However, in these studies, EC represented a minor mass fraction of PM_{10}: less than 0.4% in Viana, and 0.4% for a cobbled street and 4.6 ± 0.8% for asphalt pavements in Oporto (Alves et al., 2018, 2020). It must be considered that the high concentration of Fe in samples may have complicated the laser correction for pyrolysis. OC represented 58.2 ± 0.14% of the total carbonaceous fraction. Although samples from the asphalt street S2 presented a higher OC content, in general, the OC mass fraction in PM_{10} from the cobblestone pavement was similar to those of asphalt pavements. The sampling point with the lowest EC mass fraction was the road tunnel S6, which may be associated with the fact that heavy vehicles are not allowed inside this tunnel. Mean OC/EC and OC/TC ratios ranged between 0.60 – 5.33 and 0.37–0.84, respectively. Previous studies have reported OC/TC values ranging from 0.44 to 1.0 in Oporto and Braga (Alves et al., 2018), and from 0.70 to 0.84 in Barcelona, Zurich and Girona (Amato et al., 2011).

Table 3
PM_{10} mass fractions (wt %) of carbonaceous constituents and elements. (S1: high traffic, asphalt; S2: high traffic, cobbled; S3: high traffic, asphalt; S4: low traffic, asphalt; S5: tunnel high traffic, asphalt; S6: tunnel high traffic without heavy vehicles, asphalt).

	S1	S2	S3	S4	S5	S6
	wt %					
OC	6.58	7.21	12.8	14.6	11.7	10.0
EC	11.0	5.93	9.93	9.28	8.96	1.88
Na	0.106	0.0759	0.260	0.289	0.187	0.224
Mg	0.299	0.216	0.438	0.548	0.433	0.491
Al	1.09	0.971	1.63	1.52	1.31	1.76
Si	3.46	3.81	5.49	5.32	4.23	5.65
P	0.0497	0.0420	0.0783	0.0884	0.0660	0.0790
S	0.288	0.126	0.310	0.454	0.439	0.449
Cl	0.163	0.0778	0.248	0.331	0.183	0.282
K	0.411	0.584	0.534	0.577	0.351	0.576
Ca	12.9	8.30	10.1	12.1	9.93	11.3
Ti	0.145	0.203	0.191	0.190	0.167	0.212
V	0.00718	0.0107	0.00716	0.00871	0.0119	0.0130
Cr	0.0209	0.00854	0.0185	0.0180	0.0620	0.0397
Mn	0.0387	0.0307	0.0335	0.0332	0.0934	0.0669
Fe	3.45	2.25	3.15	2.99	9.66	6.42
Ni	0.00163	0.00200	0.00268	0.00263	0.00413	0.00357
Cu	0.0808	0.0345	0.0665	0.0641	0.262	0.166
Zn	0.121	0.0752	0.137	0.203	0.270	0.229
As	<0.000887	0.00191	0.00322	0.00131	0.00174	0.00183
Se	<0.000855	<0.000662	<0.000865	<0.000938	<0.00116	<0.000968
Br	<0.000920	<0.000641	0.00196	0.00183	<0.00203	<0.00169
Rb	0.0224	0.0222	0.00418	0.00326	0.0677	0.0480
Sr	<0.00322	<0.00163	<0.00430	<0.00454	<0.00800	<0.00544
Y	0.0102	0.00643	<0.00474	<0.00354	<0.00538	0.00986
Zr	0.0180	0.0144	<0.00672	<0.00693	0.0450	0.0322
Mo	<0.00268	0.00236	<0.00842	<0.0117	0.00856	0.00794
Ba	0.0413	<0.00267	<0.00380	0.0622	0.167	0.0847
Pb	<0.00305	0.00972	<0.00376	<0.00353	<0.00475	<0.00397
∑ TC	17.6	14.5	22.9	23.2	18.9	11.9
∑ elements	22.3	16.9	22.7	24.8	27.9	28.1

< bdl (below the detection limit)

3.3. Pollution indexes

The calculation of the enrichment factor (Fig. S1) for each element allowed to assess the intensity of road dust contamination by anthropogenic sources. The elements with minimal enrichments (*EnF* lower than 2) were Na, Mg, Si and K. S and Ca were very enriched in relation to the soil, while Cr, Cu, Zn, As and Mo presented extremely high enrichments, indicating that PM_{10} road dust is highly contaminated by anthropogenic sources. Normally, calcium is associated with crustal matter, but the high enrichment factor (average of $EnF_{Ca} = 21.3$) is indicative of anthropogenic contributions. Analysis of individual particles collected in Beijing and Qingdao, China, revealed a main anthropogenic origin, possibly in construction sites, where lime mainly composed of CaO and $Ca(OH)_2$ is applied (Zhang et al., 2005). In addition to the construction sites, in Lisbon, Ca may originate in the sidewalks along roads, which are made of limestone cubes. However, those studies that applied receptor modelling to apportion road dust in urban sites showed difficulties in separating the mineral and road dust source, since the bitumen of asphalt is traced by typical crustal species such as Al, Ca, Fe and V. Moreover, the chemical composition of dust varies seasonally and geographically (Amato et al., 2009a, 2009b, 2011, 2009a). Although potassium is commonly associated with biomass burning (Calvo et al., 2013), in this study its *EnF* was 1.0, which corresponds to a very low anthropogenic enrichment. It should be noted that the sampling took place in early autumn, with mild temperatures, and that residential heating with firewood is not significant in Lisbon. Thus, K can be regarded as a PM_{10}-bound earth crust element or soil tracer. The most enriched elements were Cu and Zn ($EnF = 440$ and 184, respectively). Previous studies have shown that these elements are present in particles from brake wear as they are part of the brake linings composition (Grigoratos and Martini, 2015; Hagino et al., 2016; Jeong, 2022; Sommer et al., 2018). Zinc alloy and galvanized components are widely used in motor vehicles, so the wear and tear of vulcanized vehicle tyres and corrosion of galvanized automobile parts may be the main source of Zn in urban environments (Jeong, 2022; Sommer et al., 2018; Zhao et al., 2015). Alves et al. (2020) documented Zn as a dominant element in PM_{10} resulting from the interaction between pavements and tyres, accounting for mass fractions of 2162 ± 1151 μg g^{-1}. Hulskotte et al. (2014) reported that Cu represented about 11.2% of brake pads. In the USA, the Cu content in brake pads will be reduced to 5% in 2021 and to 0.5% by 2025, but the measure may not be followed in other countries, where huge compositional differences can be encountered. Sulfur was also found to be an enriched element. It is present in lubricants. The S content of lubricant oil is typically higher than that of fuel by an order of magnitude or more. In automotive brake pad materials, the metal sulfides act as a solid lubricant at low and medium temperatures (Sathickbasha et al., 2019). The chemical elements Sb and Sn have not been analysed in PIXE, but it has been shown in previous studies that these metals are present in brake wear and are associated with toxicological responses (Von Uexküll et al., 2005).

PI index allowed to assess the level of contamination of metals in the thoracic fraction of road dust. Table 4 shows the results of *PI* values for each element in each sampling location. As expected, this index has yielded similar findings to those obtained with the enrichment factors, given that geochemical background values are taken in the calculations. Mineral dust elements, namely Al, Si, Ti, Mn, Mg and K, presented a low *PI,* while elements such as Cr, As and Br exhibited very high values. Cu, Zn and Mo were extremely contaminated. Cu revealed the highest *PI* value (mean $PI_{Cu} = 78.6$). Alves et al. (2020) reported similar results of *PI,* highlighting the contamination of the road dust sampled in the North of Portugal with Cu, Zn and As. In this study, As presented a mean value of $PI = 10.0$, so it is classified as being very highly contaminated. As is used in alloys of lead (e.g., car batteries) and in the processing of glass, textiles, metal adhesives, semiconductor electronic devices and is part of

Table 4
Pollution Index (*PI*) of each element in each sampling site. (S1: high traffic, asphalt; S2: high traffic, cobbled; S3: high traffic, asphalt; S4: low traffic, asphalt; S5: tunnel high traffic, asphalt; S6: tunnel high traffic without heavy vehicles, asphalt).

	PI						
	S1	S2	S3	S4	S5	S6	$\bar{X}$
Na	0.0413	0.0296	0.101	0.113	0.0727	0.0871	0.741
Mg	0.222	0.160	0.324	0.405	0.321	0.363	0.299
Al	0.141	0.125	0.210	0.196	0.169	0.227	0.178
Si	0.114	0.126	0.181	0.175	0.139	0.186	0.154
P	0.747	0.632	1.18	1.33	0.993	1.19	1.01
S	3.03	1.33	3.26	4.77	4.61	4.71	3.61
Cl	2.55	1.22	3.87	5.18	2.86	4.41	3.35
K	0.143	0.204	0.186	0.201	0.123	0.201	0.176
Ca	4.39	2.82	3.44	4.09	3.37	3.82	3.66
Ti	0.465	0.650	0.614	0.609	0.537	0.680	0.593
V	1.35	2.01	1.35	1.64	2.24	2.46	1.84
Cr	5.97	2.44	5.27	5.15	17.7	11.3	7.98
Mn	0.733	0.583	0.636	0.630	1.77	1.27	0.937
Fe	1.12	0.729	1.02	0.969	3.13	2.08	1.51
Ni	0.877	1.07	1.44	1.42	2.22	1.92	1.49
Cu	56.5	24.1	46.5	44.8	183	116	78.6
Zn	23.3	14.5	26.3	38.9	51.8	44.0	33.1
As	-	9.53	16.1	6.56	8.68	9.16	10.0
Br	-	-	12.3	11.4	-	-	11.9
Rb	2.04	2.02	0.380	0.296	6.16	4.36	2.54
Y	4.93	3.11	-	-	-	4.76	4.27
Zr	0.760	0.609	-	-	1.90	1.36	1.16
Mo	-	16.8	-	-	61.1	56.7	44.9
Ba	0.619	-	-	0.931	2.50	1.27	1.33
Pb	-	5.72	-	-	-	-	5.72

Scale	Colour	Description
< 1		Low
[1,3[		Moderate
[3,6[		Considerable
[6,12[		Very high
≥ 12		Extremely high

Table 5
Eri for heavy metal in each sampling site. (S1: high traffic, asphalt; S2: high traffic, cobbled; S3: high traffic, asphalt; S4: low traffic, asphalt; S5: tunnel high traffic, asphalt; S6: tunnel high traffic without heavy vehicles, asphalt).

	Eri						
	S1	S2	S3	S4	S5	S6	$\bar{X}$
As	-	95.3	161	65.6	86.8	91.6	100
Cu	283	121	233	224	917	581	393
Ni	4.39	5.36	7.20	7.08	11.1	9.59	7.45
Pb	-	28.6	-	-	-	-	28.6
Cr	11.9	4.88	10.5	10.3	35.4	22.7	16.0
V	2.71	4.03	2.70	3.29	4.48	4.91	3.69
Zn	23.3	14.5	26.3	38.9	51.8	44.0	33.1
Mn	0.733	0.583	0.636	0.630	1.77	1.27	0.937
Ba	0.619	-	-	0.931	2.50	1.27	1.33

Legend		
Scale	Colour	Description
< 40		Low
[40,80[		Moderate
[80,160[		Considerable
[160,320[		High
≥ 320		Very high

the herbicides used in agriculture (Alves et al., 2020; and references therein). This latter source of As may be the reason why values were much higher in some streets of Viana do Castelo, located in the vicinities of farms (*PI* = 50.1) (Alves et al., 2020; and references therein).

Regarding the integrated pollution load index of each sampling site, *PLI* varied from 1.11 to 2.32, taking into account all elements analysed. The sampling sites S1 to S4 were classified as unpolluted to moderately polluted, while road tunnels (S5 and S6) were categorized as moderately polluted.

Table 5 shows the value of the potential ecological risk factor of As, Cu, Ni, Pb, Cr, V, Zn, Mn and Ba. Only Cu represented, on average, a very high potential harmful effect (*Eri* = 393), followed by As with a considerable risk. Among the six sampled locations, the two sites that stood out with very high *Eri* of Cu were the road tunnels (S5 and S6). Road dust from these road infrastructures showed a higher mass fraction of major and trace elements (S5 = 27.9% and S6 = 28.1%) compared to the other sampling sites (16.9–24.8%): Higher Cu and Zn mass fractions were also observed in samples collected from the pavement of the two road tunnels. This may be because inside road tunnels, there is less dispersion of vehicle emissions compared to other outdoor roads.

The mean *RI* value of 543 represented a considerable risk, for which about 72.3% was due to the contribution of Cu. Alves et al. (2020) also analysed this parameter in Viana do Castelo and the pollutant of highest concern was Sn, followed by Cd and Cu. Unfortunately, Sn and Cd were not analysed in this study, which can lead to greater overvaluation of Cu. Inside the tunnels, due to the very high *Eri*, the *RI* was ≥ 600, denoting a

Table 6
TCR of carcinogenic metals for adults and children in each sampling site. (S1: high traffic, asphalt; S2: high traffic, cobbled; S3: high traffic, asphalt; S4: low traffic, asphalt; S5: tunnel high traffic, asphalt; S6: tunnel high traffic without heavy vehicles, asphalt).

	TCR adult						*TCR* children					
	S1	S2	S3	S4	S5	S6	S1	S2	S3	S4	S5	S6
As	-	2.3E-4	3.9E-4	1.6E-4	2.1E-4	2.2E-4	-	1.5E-3	2.5E-3	1.0E-3	1.4E-3	1.4E-3
Cr	6.2E-6	2.5E-6	5.4E-6	5.3E-6	1.8E-5	1.2E-5	6.2E-6	2.5E-6	5.4E-6	5.3E-6	1.8E-5	1.2E-5
Ni	9.6E-9	1.2E-8	1.6E-8	1.6E-8	2.4E-8	2.1E-8	9.6E-9	1.2E-8	1.6E-8	1.6E-8	2.4E-8	2.1E-8
Pb	-	9.4E-4	-	-	-	-	-	9.8E-4	-	-	-	-

Legend		
Scale	Colour	Description
< 1E-6		Negligible
[1E-6,1E-4[		Acceptable or Tolerable
≥ 1E-4		Harmful

high potential ecological risk.

3.4. Human health risk

The carcinogenic risk was calculated for the metals As, Cr, Ni and Pb (Table 6). The three different exposure pathways (inhalation, ingestion and dermal) were assessed for As, the ingestion and dermal routes for Pb and the inhalation route for Ni and Cr. *TCR* was higher than 1E−4 for As and Pb in the roadways where these metals were detected, suggesting that exposure to these hazardous constituents may constitute a potential carcinogenic risk for adults and children and the possibility of developing cancer over a lifetime. Lead is a highly toxic heavy metal that can affect every organ system and cause adverse health effects such as renal disease, hypertension and other cardiovascular outcomes (Sanders et al., 2009). Arsenic is a carcinogen that can cause lung and skin cancer (Ratnaike, 2003). The TCR_{Ni} for adults was lower than 1E−6, so the total cancer risk can be considered insignificant. The remaining values (TCR_{Cr} in adults and children and TCR_{Ni} in children) ranged between 1E−6 and 1E−4, indicating acceptable or tolerable cancer risks for Cr. *TCR* values are higher in children since they are a more susceptible group to exposure to air pollution (Buka et al., 2006; Holst et al., 2020; Prunicki et al., 2021).

In terms of non-carcinogenic risk, ingestion of dust particles appears to be the route of exposure to road dust that results in a higher risk for all elements (Table 7). The *PEF* was developed for contaminated background soil grains that are more cohesive than road dust. Thus, the results for the inhalation route may be underestimated because the concentration of trace elements in inhaled air can be higher since road dust is more easily resuspended (Ferreira-Baptista and De Miguel, 2005). The hazard index (*HI*), which is the sum of the three exposure pathways, suggested that there was no significant non-carcinogenic risks for adults posed by As, Zn, Cu, Pb, Cr, Ni, Mn, Fe, Al, Ba, Mo and V, since *HQ* was much lower than 1. In specific streets, children are potentially more susceptible to the health effects from exposure to metals in S3 by As ($HI_{As} = 1.1$) and in canyon-like roadways with little dispersion, such as tunnels, by Cr ($HI_{Cr} = 2.1$ in S5 and $HI_{Cr} = 1.3$ in S6) and by Fe ($HI_{Fe} = 1.4$ in S5), since values were higher than the "safe" level ($HI = 1$). Comparable results were obtained in Viana do Castelo, where it was found that *HI* was within safe values for adults, but children were potentially more susceptible to exposure to some elements, including As, Fe and Cr (Alves et al., 2020). In Luanda, Ferreira-Baptista and De Miguel (2005) also recorded HI_{As} and $HI_{Pb} > 0.1$, with $HI_{Pb} = 0.72$. Children's exposure to Pb in large enough doses can trigger neurological and developmental disorders (Sanders et al., 2009).

4. Conclusions

This study encompassed the first road dust monitoring campaign ever carried out in Lisbon. Results showed that PM_{10} resulting from the resuspension of road dust contains several hazardous chemical constituents that can trigger potential effects on human health. Cu presented the highest pollution index in all road sampling sites and the highest potential harmful effect, followed by As. Exposure to As may constitute a potential carcinogenic risk for adults and children, since *TCR* was higher than 1E-4 in 90% of the sampling sites, suggesting the possibility of developing cancer over a lifetime. In cobbled pavement, Pb also represented a potential carcinogenic risk for adults and children. Thus, further studies involving non-exhaust particulate contaminants and their toxicological properties in other roads and cities are needed to generate more reliable and representative results.

This new data set can contribute to European emission inventories and may help to increase the completeness of the SPECIEUROPE database. The new source chemical profiles can be useful to apply receptor models and more accurately estimate the contribution of road dust to the PM_{10} atmospheric levels. In addition, the information obtained in this study can also be used to help decision-making by local governments to implement air quality management for urban PM_{10}.

CRediT authorship contribution statement

I. Cunha-Lopes: Conceptualization, Methodology, Formal analysis, Investigation, Writing – original draft, Writing – review & editing,

Table 7
Average ± SD of *HQ* by ingestion, inhalation and dermal and *HI* for adults and children.

	HQing		*HQinh*		*HQdermal*		$HI = \sum HQ_i$	
	Average ± SD							
	Adult	Children	Adult	Children	Adult	Children	Adult	Children
As	9.5E-2 ± 3.1E-2	6.7E-1 ± 2.1E-1	9.0E-9 ± 2.9E-9	1.9E-8 ± 6.0E-9	2.2E-5 ± 7.0E-6	8.0E-6 ± 2.6E-6	9.5E-2 ± 3.1E-2	6.7E-1 ± 2.1E-1
Zn	8.2E-3 ± 3.2E-3	5.7E-2 ± 2.2E-2	7.7E-7 ± 3.0E-7	1.6E-6 ± 6.3E-7	1.9E-3 ± 7.3E-4	6.9E-4 ± 2.7E-4	1.0E-2 ± 3.9E-3	5.8E-2 ± 2.3E-2
Cu	4.0E-2 ± 2.8E-2	2.8E-1 ± 2.0E-1	3.8E-6 ± 2.6E-6	7.8E-6 ± 5.5E-6	4.1E-3 ± 2.8E-3	1.5E-3 ± 1.0E-3	4.4E-2 ± 3.1E-2	2.8E-1 ± 2.0E-1
Pb	9.9E-2	6.9E-1	3.7E-6	7.7E-6	8.1E-3	3.0E-3	1.1E-1	7.0E-1
Cr	1.3E-1 ± 8.5E-2	9.3E-1 ± 5.9E-1	1.3E-3 ± 8.4E-4	2.7E-3 ± 1.8E-3	4.0E-3 ± 2.6E-3	1.5E-3 ± 9.5E-4	1.4E-1 ± 8.8E-2	9.4E-1 ± 6.0E-1
Ni	2.0E-3 ± 6.1E-4	1.4E-2 ± 4.3E-3	1.8E-7 ± 5.6E-8	3.8E-7 ± 1.2E-7	2.2E-4 ± 6.9E-5	8.2E-5 ± 2.5E-5	2.2E-3 ± 6.8E-4	1.4E-2 ± 4.3E-3
Mn	1.5E-2 ± 7.2E-3	1.1E-1 ± 5.0E-2	4.6E-3 ± 2.2E-3	9.7E-3 ± 4.5E-3	1.2E-2 ± 5.5E-3	4.3E-3 ± 2.0E-3	3.2E-2 ± 1.5E-2	1.2E-1 ± 5.7E-2
Fe	9.5E-2 ± 5.3E-2	6.6E-1 ± 3.7E-1	–	–	–	–	9.5E-2 ± 5.3E-2	6.6E-1 ± 3.7E-1
Al	5.8E-3 ± 1.6E-3	4.0E-2 ± 1.1E-2	3.8E-4 ± 1.1E-4	7.9E-4 ± 2.2E-4	1.8E-3 ± 4.9E-4	6.5E-4 ± 1.8E-4	7.9E-3 ± 2.2E-3	4.2E-2 ± 1.2E-2
Ba	1.8E-2 ± 9.8E-3	1.3E-1 ± 6.8E-2	8.4E-4 ± 4.5E-4	1.7E-3 ± 9.4E-4	7.9E-3 ± 4.2E-3	2.9E-3 ± 1.6E-3	2.7E-2 ± 1.4E-2	1.3E-1 ± 7.1E-2
Mo	1.8E-2 ± 8.0E-3	1.3E-1 ± 5.6E-2	–	–	1.4E-3 ± 6.4E-4	5.3E-4 ± 2.3E-4	1.9E-2 ± 8.6E-3	1.3E-1 ± 5.6E-2
V	2.0E-2 ± 4.6E-3	1.4E-1 ± 3.2E-2	1.9E-6 ± 4.3E-7	3.9E-6 ± 9.0E-7	6.1E-4 ± 1.4E-4	2.2E-4 ± 5.1E-5	2.1E-2 ± 4.7E-3	1.4E-1 ± 3.2 E−2

Visualization. **C.A. Alves:** Conceptualization, Methodology, Resources, Writing – review & editing, Supervision, Project administration, Funding acquisition. **I. Casotti Rienda:** Investigation, Writing – review & editing. **T. Faria:** Investigation, Writing – review & editing. **F. Lucarelli:** Resources. **X. Querol:** Resources. **F. Amato:** Methodology, Resources. **S. M. Almeida:** Conceptualization, Methodology, Investigation, Resources, Writing – review & editing, Supervision, Project administration.

Declaration of competing interest

The authors declare that they have no known competing financial interests or personal relationships that could have appeared to influence the work reported in this paper.

Acknowledgements

Inês Lopes and Ismael Casotti Rienda acknowledge their PhD fellowships (SFRH/BD/147074/2019 and SFRH/BD/144550/2019, respectively) from the Portuguese Foundation for Science and Technology (FCT). The sampling campaign and analytical work were supported by the project "SOPRO: Chemical and toxicological SOurce PROfiling of particulate matter in urban air", POCI-01-0145-FEDER-029574, funded by FEDER, through COMPETE2020 - Programa Operacional Competitividade e Internacionalização (POCI), and by national funds (OE), through FCT/MCTES. Thanks are also due to RADIATE (H2020, #824096). We are grateful for the support to CESAM (UIDB/50017/2020 & UIDP/50017/2020), to FCT/MCTES through national funds, and co-funding by FEDER, within the PT2020 Partnership Agreement and Compete 2020. Authors also gratefully acknowledge the FCT support through the UIDB/04349/2020 project. An acknowledgment is also given to António Almeida from EMEL, Pedro Ladeira from the Lisbon City Council and the Municipal Police of Lisbon, for all the logistic support.

Appendix A. Supplementary data

Supplementary data to this article can be found online at https://doi.org/10.1016/j.atmosenv.2022.119221.

References

Adimalla, N., 2020. Heavy metals contamination in urban surface soils of Medak province, India, and its risk assessment and spatial distribution. Environ. Geochem. Health 42, 59–75. https://doi.org/10.1007/s10653-019-00270-1.

Almeida, S.M., Freitas, M.C., Repolho, C., Dionísio, I., Dung, H.M., Pio, C.A., Alves, C., Caseiro, A., Pacheco, A.M.G., 2009. Evaluating children exposure to air pollutants for an epidemiological study. J. Radioanal. Nucl. Chem. 280, 405–409. https://doi.org/10.1007/s10967-009-0535-3.

Almeida, S.M., Pio, C.A., Freitas, M.C., Reis, M.A., Trancoso, M.A., 2006. Approaching PM2.5 and PM2.5 - 10 source apportionment by mass balance analysis, principal component analysis and particle size distribution. Sci. Total Environ. 368, 663–674. https://doi.org/10.1016/j.scitotenv.2006.03.031.

Almeida, S.M., Pio, C.A., Freitas, M.C., Reis, M.A., Trancoso, M.A., 2005. Source apportionment of fine and coarse particulate matter in a sub-urban area at the Western European Coast. Atmos. Environ. 39, 3127–3138.

Almeida, S.M., Silva, A.V., Sarmento, S., 2014. Effects of exposure to particles and ozone on hospital admissions for cardiorespiratory diseases in SetúBal, Portugal. J. Toxicol. Environ. Health Part A Curr. Issues 77, 837–848. https://doi.org/10.1080/15287394.2014.887399.

Alves, C.A., Evtyugina, M., Vicente, A.M.P., Vicente, E.D., Nunes, T.V., Silva, P.M.A., Duarte, M.A.C., Pio, C.A., Amato, F., Querol, X., 2018. Chemical profiling of PM10 from urban road dust. Sci. Total Environ. 634, 41–51. https://doi.org/10.1016/j.scitotenv.2018.03.338.

Alves, C.A., Vicente, E.D., Vicente, A.M.P., Rienda, I.C., Tomé, M., Querol, X., Amato, F., 2020. Loadings, chemical patterns and risks of inhalable road dust particles in an Atlantic city in the north of Portugal. Sci. Total Environ. 737 https://doi.org/10.1016/j.scitotenv.2020.139596.

Amato, F., Alastuey, A., Karanasiou, A., Lucarelli, F., Nava, S., Calzolai, G., Severi, M., Becagli, S., Gianelle, V.L., Colombi, C., Alves, C., Custódio, D., Nunes, T., Cerqueira, M., Pio, C., Eleftheriadis, K., Diapouli, E., Reche, C., Minguillón, M.C., Manousakas, M.I., Maggos, T., Vratolis, S., Harrison, R.M., Querol, X., 2016a. AIRUSE-LIFE+: a harmonized PM speciation and source apportionment in five southern European cities. Atmos. Chem. Phys. 16, 3289–3309. https://doi.org/10.5194/acp-16-3289-2016.

Amato, F., Bedogni, M., Padoan, E., Querol, X., Ealo, M., Rivas, I., 2017. Characterization of road dust emissions in milan: impact of vehicle fleet speed. Aerosol Air Qual. Res. 17, 2438–2449. https://doi.org/10.4209/aaqr.2017.01.0017.

Amato, F., Nava, S., Lucarelli, F., Querol, X., Alastuey, A., Baldasano, J.M., Pandolfi, M., 2010. A comprehensive assessment of PM emissions from paved roads: real-world Emission Factors and intense street cleaning trials. Sci. Total Environ. 408, 4309–4318. https://doi.org/10.1016/j.scitotenv.2010.06.008.

Amato, F., O, F., Pandolfi, M., Alastuey, A., Querol, X., Moukhtar, S., Bruge, B., Verlhac, S., Orza, J.A.G., Bonnaire, N., Le Priol, T., Petit, J.F., Sciare, J., 2016b. Traffic induced particle resuspension in Paris: emission factors and source contributions. Atmos. Environ. 129, 114–124. https://doi.org/10.1016/j.atmosenv.2016.01.022.

Amato, F., Pandolfi, M., Escrig, A., Querol, X., Alastuey, A., Pey, J., Perez, N., Hopke, P. K., 2009a. Quantifying road dust resuspension in urban environment by Multilinear Engine: a comparison with PMF2. Atmos. Environ. 43, 2770–2780. https://doi.org/10.1016/j.atmosenv.2009.02.039.

Amato, F., Pandolfi, M., Moreno, T., Furger, M., Pey, J., Alastuey, A., Bukowiecki, N., Prevot, A.S.H., Baltensperger, U., Querol, X., 2011. Sources and variability of inhalable road dust particles in three European cities. Atmos. Environ. 45, 6777–6787. https://doi.org/10.1016/j.atmosenv.2011.06.003.

Amato, F., Pandolfi, M., Viana, M., Querol, X., Alastuey, A., Moreno, T., 2009b. Spatial and chemical patterns of PM10 in road dust deposited in urban environment. Atmos. Environ. 43, 1650–1659. https://doi.org/10.1016/j.atmosenv.2008.12.009.

ASF, 2020. Parque automóvel seguro 2020 [WWW Document]. URL. https://www.asf.com.pt/NR/exeres/7D383D46-9431-416E-98C7-395B0A9E7080.htm, 9.30.21.

Buka, I., Koranteng, S., Osornio-Vargas, A.R., 2006. The Effects of Air Pollution on the Health of Children. Paediatr. Child Health, Oxford. https://doi.org/10.1093/pch/11.8.513.

Bukowiecki, N., Lienemann, P., Hill, M., Furger, M., Richard, A., Amato, F., Prévôt, A.S. H., Baltensperger, U., Buchmann, B., Gehrig, R., 2010. PM10 emission factors for non-exhaust particles generated by road traffic in an urban street canyon and along a freeway in Switzerland. Atmos. Environ. https://doi.org/10.1016/j.atmosenv.2010.03.039.

Byčenkiene, S., Plauškaite, K., Dudoitis, V., Ulevicius, V., 2014. Urban background levels of particle number concentration and sources in Vilnius, Lithuania. Atmos. Res. 143, 279–292. https://doi.org/10.1016/j.atmosres.2014.02.019.

Calvo, A.I., Alves, C.A., Castro, A., Pont, V., Vicente, A.M., Fraile, R., 2013. Research on aerosol sources and chemical composition: past, current and emerging issues. Atmos. Res. 120–121, 1–28. https://doi.org/10.1016/j.atmosres.2012.09.021.

Calzolai, G., Nava, S., Lucarelli, F., Chiari, M., Giannoni, M., Becagli, S., Traversi, R., Marconi, M., Frosini, D., Severi, M., Udisti, R., Di Sarra, A., Pace, G., Meloni, D., Bommarito, C., Monteleone, F., Anello, F., Sferlazzo, D.M., 2015. Characterization of PM10 sources in the central Mediterranean. Atmos. Chem. Phys. 15, 13939–13955. https://doi.org/10.5194/acp-15-13939-2015.

Campbell, J.L., Boyd, N.I., Grassi, N., Bonnick, P., Maxwell, J.A., 2010. The Guelph PIXE software package IV. Nucl. Instrum. Methods Phys. Res. Sect. B Beam Interact. Mater. Atoms 268, 3356–3363. https://doi.org/10.1016/j.nimb.2010.07.012.

Candeias, C., Vicente, E., Tomé, M., Rocha, F., Ávila, P., Alves, C., 2020. Geochemical, mineralogical and morphological characterisation of road dust and associated health risks. Int. J. Environ. Res. Publ. Health 17. https://doi.org/10.3390/ijerph17051563.

Casotti Rienda, I., Alves, C.A., 2021. Road dust resuspension: a review. Atmos. Res. 261, 105740 https://doi.org/10.1016/j.atmosres.2021.105740.

Chen, H., Teng, Y., Lu, S., Wang, Y., Wang, J., 2015. Contamination features and health risk of soil heavy metals in China. Sci. Total Environ. https://doi.org/10.1016/j.scitotenv.2015.01.025.

Cho, H.K., Park, C.G., Shin, H.J., Park, K.H., Lim, H. Bin, 2018. Comparison of the in vitro toxicological activity of various particulate matter. Toxicol. Ind. Health 34, 99–109. https://doi.org/10.1177/0748233717749694.

Custódio, D., Cerqueira, M., Alves, C., Nunes, T., Pio, C., Esteves, V., Frosini, D., Lucarelli, F., Querol, X., 2016. A one-year record of carbonaceous components and major ions in aerosols from an urban kerbside location in Oporto. Portugal. Sci. Total Environ. 562, 822–833. https://doi.org/10.1016/j.scitotenv.2016.04.012.

Diapouli, E., Manousakas, M.I., Vratolis, S., Vasilatou, V., Pateraki, S., Bairachtari, K.A., Querol, X., Amato, F., Alastuey, A., Karanasiou, A.A., Lucarelli, F., Nava, S., Calzolai, G., Gianelle, V.L., Colombi, C., Alves, C., Custódio, D., Pio, C., Spyrou, C., Kallos, G.B., Eleftheriadis, K., 2017. AIRUSE-LIFE +: estimation of natural source contributions to urban ambient air PM10 and PM2. 5 concentrations in southern Europe - implications to compliance with limit values. Atmos. Chem. Phys. 17, 3673–3685. https://doi.org/10.5194/acp-17-3673-2017.

Dumax-Vorzet, A.F., Tate, M., Walmsley, R., Elder, R.H., Povey, A.C., 2015. Cytotoxicity and genotoxicity of Urban particulate matter in mammalian cells. Mutagenesis. https://doi.org/10.1093/mutage/gev025.

EEA, 2019. Air Quality in Europe — 2019 Report — EEA Report No 10/2019. Luxembourg: Publications Office of the European Union.

EEA, 2020. Air Quality in Europe — 2020 Report — EEA Report No 9/2020. Luxembourg: Publications Office of the European Union.

EU, 2008. Diretiva 2008/50/CE - Relativa à qualidade do ar ambiente e a um ar mais limpo na Europa.

Eurostat, 2016. Urban Europe, the European Territory. https://doi.org/10.4324/9781315777962-2. Luxembourg.

Farwick zum Hagen, F.H., Mathissen, M., Grabiec, T., Hennicke, T., Rettig, M., Grochowicz, J., Vogt, R., Benter, T., 2019. On-road vehicle measurements of brake

wear particle emissions. Atmos. Environ. 217, 116943 https://doi.org/10.1016/j.atmosenv.2019.116943.
Ferreira-Baptista, L., De Miguel, E., 2005. Geochemistry and risk assessment of street dust in Luanda, Angola: a tropical urban environment. Atmos. Environ. 39, 4501–4512. https://doi.org/10.1016/j.atmosenv.2005.03.026.
Grigoratos, T., Martini, G., 2015. Brake wear particle emissions: a review. Environ. Sci. Pollut. Res. 22, 2491–2504. https://doi.org/10.1007/s11356-014-3696-8.
Gustafsson, M., Blomqvist, G., Järlskog, I., Lundberg, J., Janhäll, S., Elmgren, M., Johansson, C., Norman, M., Silvergren, S., 2019. Road dust load dynamics and influencing factors for six winter seasons in Stockholm, Sweden. Atmos. Environ. X 2. https://doi.org/10.1016/j.aeaoa.2019.100014.
Hagino, H., Oyama, M., Sasaki, S., 2016. Laboratory testing of airborne brake wear particle emissions using a dynamometer system under urban city driving cycles. Atmos. Environ. https://doi.org/10.1016/j.atmosenv.2016.02.014.
Hakanson, L., 1980. An ecological risk index for aquatic pollution control.a sedimentological approach. Water Res. 14, 975–1001.
Han, L., Zhuang, G., Cheng, S., Wang, Y., Li, J., 2007. Characteristics of re-suspended road dust and its impact on the atmospheric environment in Beijing. Atmos. Environ. https://doi.org/10.1016/j.atmosenv.2007.05.044.
Holst, G.J., Pedersen, C.B., Thygesen, M., Brandt, J., Geels, C., Bønløkke, J.H., Sigsgaard, T., 2020. Air pollution and family related determinants of asthma onset and persistent wheezing in children: nationwide case-control study. BMJ. https://doi.org/10.1136/bmj.m2791.
Huang, M., Kang, Y., Wang, W., Chan, C.Y., Wang, X., Wong, M.H., 2015. Potential cytotoxicity of water-soluble fraction of dust and particulate matters and relation to metal(loid)s based on three human cell lines. Chemosphere. https://doi.org/10.1016/j.chemosphere.2015.04.004.
Hulskotte, J.H.J., Roskam, G.D., Denier van der Gon, H.A.C., 2014. Elemental composition of current automotive braking materials and derived air emission factors. Atmos. Environ. https://doi.org/10.1016/j.atmosenv.2014.10.007.
Jeong, H., 2022. Toxic metal concentrations and Cu–Zn–Pb isotopic compositions in tires. J. Anal. Sci. Technol. 13 https://doi.org/10.1186/s40543-021-00312-3.
Kelly, F.J., Fussell, J.C., 2011. Air pollution and airway disease. Clin. Exp. Allergy 41, 1059–1071. https://doi.org/10.1111/j.1365-2222.2011.03776.x.
Khan, R.K., Strand, M.A., 2018. Road dust and its effect on human health: a literature review. Epidemiol. Health. https://doi.org/10.4178/epih.e2018013.
Koh, B., Kim, E.A., 2019. Comparative analysis of urban road dust compositions in relation to their potential human health impacts. Environ. Pollut. 255 https://doi.org/10.1016/j.envpol.2019.113156.
Lee, C.S., Li, X., Shi, W., Ching-nga Cheung, S., Thornton, I., 2006. Metal contamination in urban, suburban, and country park soils of Hong Kong: a study based on GIS and multivariate statistics. Sci. Total Environ. 356, 45–61.
Legret, M., Odie, L., Demare, D., Jullien, A., 2005. Leaching of heavy metals and polycyclic aromatic hydrocarbons from reclaimed asphalt pavement. Water Res. 39, 3675–3685. https://doi.org/10.1016/j.watres.2005.06.017.
Li, H., Shi, A., Zhang, X., 2015. Particle size distribution and characteristics of heavy metals in road-deposited sediments from Beijing Olympic Park. J. Environ. Sci. (China) 32, 228–237. https://doi.org/10.1016/j.jes.2014.11.014.
Lucarelli, F., Calzolai, G., Chiari, M., Nava, S., Carraresi, L., 2018. Study of atmospheric aerosols by IBA techniques: the LABEC experience. Nucl. Instrum. Methods Phys. Res. Sect. B Beam Interact. Mater. Atoms 417, 121–127. https://doi.org/10.1016/j.nimb.2017.07.034.
Mendonça, J.L., 2016. A importância da água subterrânea no concelho de Lisboa em situação de crise extrema. https://doi.org/10.13140/RG.2.2.24988.90240.
Oroumiyeh, F., Zhu, Y., 2021. Brake and tire particles measured from on-road vehicles: effects of vehicle mass and braking intensity. Atmos. Environ. X 12, 100121. https://doi.org/10.1016/j.aeaoa.2021.100121.
Pant, P., Harrison, R.M., 2013. Estimation of the contribution of road traffic emissions to particulate matter concentrations from field measurements: a review. Atmos. Environ. 77, 78–97. https://doi.org/10.1016/j.atmosenv.2013.04.028.
Pio, C., Cerqueira, M., Harrison, R.M., Nunes, T., Mirante, F., Alves, C., Oliveira, C., Sanchez de la Campa, A., Artíñano, B., Matos, M., 2011. OC/EC ratio observations in Europe: Re-thinking the approach for apportionment between primary and secondary organic carbon. Atmos. Environ. 45, 6121–6132. https://doi.org/10.1016/j.atmosenv.2011.08.045.
Polidori, A., Turpin, B.J., Rodenburg, L.A., Maimone, F., Davidson, C.I., 2008. Organic pm2.5: fractionation by polarity, ftir spectroscopy, and om/oc ratio for the pittsburgh aerosol. Aerosol Sci. Technol. 42, 233–246. https://doi.org/10.1080/02786820801958767.
Prunicki, M., Cauwenberghs, N., Lee, J., Zhou, X., Movassagh, H., Noth, E., Lurmann, F., Hammond, S.K., Balmes, J.R., Desai, M., Wu, J.C., Nadeau, K.C., 2021. Air pollution exposure is linked with methylation of immunoregulatory genes, altered immune cell profiles, and increased blood pressure in children. Sci. Rep. 11, 1–12. https://doi.org/10.1038/s41598-021-83577-3.
Ratnaike, R.N., 2003. Acute and chronic arsenic toxicity. Postgrad. Med. 79, 391–396. https://doi.org/10.1136/pmj.79.933.391.
Sanders, T., Liu, Y., Buchner, V., Tchounwou, P.B., 2009. Neurotoxic effects and biomarkers of lead exposure: a review. Rev. Environ. Health 24, 15–45.
Sathickbasha, K., Selvakumar, A.S., Balaji, M.A.S., Rajan Surya, B., 2019. The dual role of metal sulfides as lubricant and abrasive: an interface study in friction composite. Mater. Res. Express 6.
Sommer, F., Dietze, V., Baum, A., Sauer, J., Gilge, S., Maschowski, C., Gieré, R., 2018. Tire abrasion as a major source of microplastics in the environment. Aerosol Air Qual. Res. 18, 2014–2028. https://doi.org/10.4209/aaqr.2018.03.0099.
Thorpe, A., Harrison, R.M., 2008. Sources and properties of non-exhaust particulate matter from road traffic: a review. Sci. Total Environ. 400, 270–282. https://doi.org/10.1016/j.scitotenv.2008.06.007.
USEPA, 1989. Risk assessment guidance for superfund. In: Human Health Evaluation Manual. Washingtom, DC: Office of Emergency and Remedial Response. Part A.
Von Uexküll, O., Skerfving, S., Doyle, R., Braungart, M., 2005. Antimony in brake pads-a carcinogenic component? J. Clean. Prod. 13, 19–31. https://doi.org/10.1016/j.jclepro.2003.10.008.
Watson, J.G., Chow, J.C., Pace, T.G., 2000. Fugitive dust emissions. In: John Wiley & Sons, I., Davis, W.T. (Eds.), Air Pollution Engineering Manual. New York, pp. 117–135.
Wedepohl, H.K., 1995. The composition of the continental crust. Geochem. Cosmochim. Acta 59, 1217–1232. https://doi.org/10.1016/0016-7037(95)00038-2.
Wiseman, C.L.S., Levesque, C., Rasmussen, P.E., 2021. Characterizing the sources, concentrations and resuspension potential of metals and metalloids in the thoracic fraction of urban road dust. Sci. Total Environ. 786, 147467 https://doi.org/10.1016/j.scitotenv.2021.147467.
Wu, J., Teng, Y., Lu, S., Wang, Y., Jiao, X., 2014. Evaluation of soil contamination indices in a mining area of Jiangxi, China. PLoS One 9. https://doi.org/10.1371/journal.pone.0112917.
Yang, J., Teng, Y., Song, L., Zuo, R., 2016. Tracing sources and contamination assessments of heavy metals in road and foliar dusts in a typical mining city, China. PLoS One 11, 1–19. https://doi.org/10.1371/journal.pone.0168528.
Yu, H., Zhao, X., Wang, J., Yin, B., Geng, C., Wang, X., Gu, C., Huang, L., Yang, W., Bai, Z., 2020. Chemical characteristics of road dust PM2.5 fraction in oasis cities at the margin of Tarim Basin. J. Environ. Sci. (China) 95, 217–224. https://doi.org/10.1016/j.jes.2020.03.030.
Zgłobicki, W., Telecka, M., Skupiński, S., 2019. Assessment of short-term changes in street dust pollution with heavy metals in Lublin (E Poland)—levels, sources and risks. Environ. Sci. Pollut. Res. 26, 35049–35060.
Zhang, C., Qiao, Q., Piper, J.D.A., Huang, B., 2011. Assessment of heavy metal pollution from a Fe-smelting plant in urban river sediments using environmental magnetic and geochemical methods. Environ. Pollut. https://doi.org/10.1016/j.envpol.2011.04.006.
Zhang, D., Shi, G., Iwasaka, Y., Hu, M.I.N., Zang, J., 2005. Anthropogenic Calcium Particles Observed in Beijing and Qingdao, china, pp. 261–276.
Zhang, M., Wang, H., 2009. Concentrations and chemical forms of potentially toxic metals in road-deposited sediments from different zones of Hangzhou, China. J. Environ. Sci. 21, 625–631. https://doi.org/10.1016/S1001-0742(08)62317-7.
Zhao, H., Yin, C., Chen, M., Wang, W., Chris, J., Shan, B., 2009. Size distribution and diffuse pollution impacts of PAHs in street dust in urban streams in the Yangtze River Delta. J. Environ. Sci. 21, 162–167. https://doi.org/10.1016/S1001-0742(08)62245-7.
Zhao, N., Lu, X., Chao, S., Xu, X., 2015. Multivariate statistical analysis of heavy metals in less than 100 μm particles of street dust from Xining, China. Environ. Earth Sci. 73, 2319–2327. https://doi.org/10.1007/s12665-014-3578-x.
Zhao, P., Feng, Y., Zhu, T., Wu, J., 2006. Characterizations of resuspended dust in six cities of North China. Atmos. Environ. 40, 5807–5814. https://doi.org/10.1016/j.atmosenv.2006.05.026.